

Fast clinically feasible MR sequences to map electrical tissue conductivity for improved accuracy in hyperthermia treatment planning (HTP)

Gavazzi S.,¹ Shcherbakova Y.,² Mandija S.,² AT van den Berg C.,^{1,2} JW Lagendijk J.,¹ JA Stalpers L.,³ Crezee H.,³ and LHMW van Lier A.,¹

¹Department of Radiotherapy, University Medical Center Utrecht, Utrecht, The Netherlands,

²Center for Image Sciences, University Medical Center Utrecht, Utrecht, The Netherlands,

³Department of Radiation Oncology, Academic Medical Center Amsterdam, Amsterdam, The Netherlands

Presented at ESHO, Berlin, 2018

Cite this article as:

Gavazzi S., Shcherbakova Y., Mandija S et al. (2018); Fast clinically feasible MR sequences to map electrical tissue conductivity for improved accuracy in hyperthermia treatment planning (HTP)

Oncothermia Journal 23:14-15

www.oncothermia-journal.com/journal/2018/Fast_clinically_feasible_MR.pdf

Fast clinically feasible MR sequences to map electrical tissue conductivity for improved accuracy in hyperthermia treatment planning (HTP)



Soraya Gavazzi¹, Yulia Shcherbakova², Stefano Mandija², Cornelis AT van den Berg^{1,2}, Jan JW Lagendijk¹, Lukas JA Stalpers³, Hans Crezee³, and Astrid LHMW van Lier¹

¹Department of Radiotherapy, University Medical Center Utrecht, Utrecht, The Netherlands. ²Center for Image Sciences, University Medical Center Utrecht, Utrecht, The Netherlands. ³Department of Radiation Oncology, Academic Medical Center Amsterdam, Amsterdam, The Netherlands

INTRODUCTION

- Electrical properties for hyperthermia treatment planning (HTP) are measurable MRI using Electrical Property Tomography (EPT)¹⁻⁴.
- EPT-based patient-specific conductivity σ values:
 - have a significant impact on reliability of HTP⁴.
 - are based on transceive phase (Φ^{\pm}) measurement, typically measured with a **time-consuming** spin-echo (SE) sequence¹

Purpose: To investigate faster alternatives for Φ^{\pm} -mapping

Study design: **bSSFP**⁵ sequence and **PLANET**⁶, an ellipse fitting approach on phase-cycled bSSFP data are compared to SE, based on precision, acquisition speed and quality of reconstructed conductivity maps in a phantom and a healthy brain.

METHODS

MR measurements

- 3T (Philips Ingenia, The Netherlands)
- Transmit: body coil
- Receive: 15-channel head coil
- Cylindrical phantom content: H₂O + 5.1 g/L NaCl + 2% agar with $\sigma = 0.80$ S/m
- In vivo:* brain of a healthy volunteer.

Analysis on transceive phase

- Precision \rightarrow SD(Φ^{\pm}) in ROI. SD(Φ^{\pm}) corresponds to RMSE of 2D parabolic fitting to measured Φ^{\pm} ⁷
- Efficiency $\rightarrow 1 / (\text{SD}(\Phi^{\pm}) \cdot \text{scan duration})$

Conductivity reconstruction²

- "phase-only EPT"
- transceive phase assumption

Analysis on conductivity

- Accuracy \rightarrow Mean(σ) in ROI.
- Precision \rightarrow SD(σ) in ROI.

	SE					PLANET					bSSFP				
FOV (mm ²)	240 x 240 x 60					240 x 240 x 60					240 x 240 x 60				
Imaging mode	2D Multi-slice					3D					3D				
Phase-cycling scheme	N.A.					bSSFP with 8 cycles, phase increment = 45°					N.A.				
Imaging flip angle (°)	90					25					25				
Resolution (mm)	1.5	1.88	2.5	3	3.75	1.5	1.88	2.5	3	3.75	1.5	1.88	2.5	3	3.75
TE (ms)	5.2					4.6					4.6				
TR (ms)	1000	850	675	615	615	4.6					4.6				
Scan duration (min:sec)	10:52	7:26	4:28	3:25	2:46	7:43	4:53	2:46	2:00	1:13	00:58	00:37	00:21	00:15	00:09

Table 1: Sequence settings for phantom and *in vivo* MR measurements. Isotropic resolutions used.

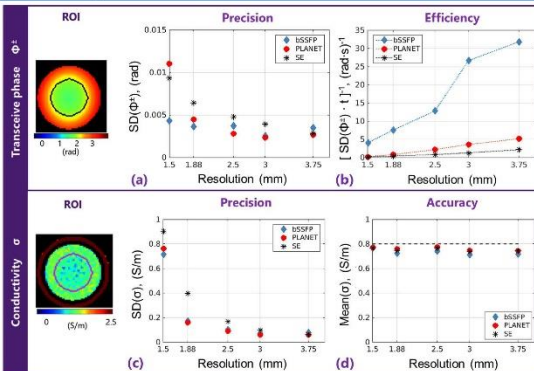


Figure 1: Analysis results on transceive phase and conductivity for SE, bSSFP and PLANET. (a) Precision of the transceive phase (b) Sequence efficiency (c) Precision of the conductivity (d) Accuracy of the conductivity

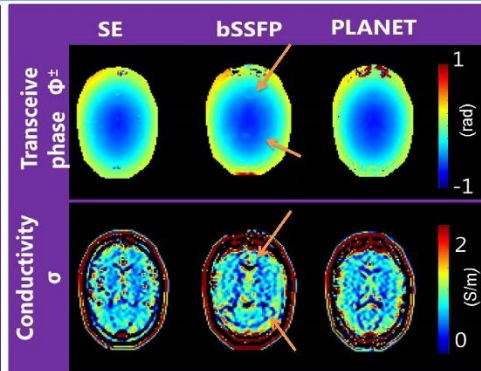


Figure 2: Maps of the transceive phase (1st row) and the conductivity (2nd row) for the three sequences: SE (1st column), bSSFP (2nd column) and PLANET (3rd column). Isotropic resolution: 2.5 mm.

RESULTS

All three techniques had similar precision performances with respect to Φ^{\pm} (Fig. 1a). However, bSSFP was the most time-efficient technique (Fig. 1b) (14-24 times more efficient than SE). PLANET was 1.2-2.8 times more efficient than SE.

Mean conductivity values were slightly biased from the true values, as expected when a "phase-only" EPT reconstruction is used (Fig. 1d). The greatest bias of 10% was found for bSSFP-based conductivity. Precision in conductivity was comparable for bSSFP and PLANET for all resolutions (Fig. 1c). For the resolution typically used in EPT, i.e. 2.5 mm, the precision in the conductivity approximated 12% of the true value for bSSFP and PLANET and almost 24% for SE. Standard deviation values for all the techniques doubled when the resolution was increased from 2.5 mm to 1.88 mm.

In vivo results are based on 2.5 mm resolution scans for all techniques (Fig. 2).

The bSSFP Φ^{\pm} -map was mildly corrupted by local B_0 field variations, that were amplified in the reconstructed σ -map (see orange arrows in Fig. 2)

PLANET showed less sensitivity to these variations and was faster than SE. Moreover, PLANET-based σ resembled the σ reconstructed on SE data.

DISCUSSION

bSSFP is the most time-efficient method for conductivity mapping (Fig. 1) but small local B_0 field variations affecting its phase pattern in the brain altered the apparent brain conductivity distribution (Fig. 2).

PLANET intrinsically corrected for these local field variations and the PLANET-based conductivity resembled the conductivity obtained with SE in the brain. PLANET was also increasingly faster than SE when resolution was increased. For an isotropic resolution of 2 mm, typically used for HTP, the standard deviation of the conductivity reconstructed on SE data was ~50% of the true conductivity value, versus ~25% when conductivity was obtained from bSSFP and PLANET acquisitions (with shorter scan durations).

CONCLUSION

PLANET showed to be a good candidate to image brain conductivity and could potentially replace SE in the imaging protocol for MR-based HTP. As a bonus, PLANET reconstructs simultaneously quantitative T_1 , T_2 , B_0 maps⁸.

REFERENCES

- Katscher et al. IEEE Trans Med Imaging. 2009;28(9):1365-74
- van Lier et al. Magn Reson Med. 2012;67(2):552-61
- Crezee et al. 1st IEEE IMBIOC; 2017, p. 1-4
- Balidemaj et al. Int J Hyperthermia. 2016;32(5):558-68
- Stehning et al. Proc 20th ISMRM. 2012;386
- Shcherbakova et al. Magn Reson Med. 2017;0:1-12
- Katscher et al. Proc 20th ISMRM. 2012; 3482